SCIENCE LETTERS

ISSN: 1675-7785
eISSN: 2682-8626

Available online at
https://scilett-fsg.uitm.edu.my/

Science Letters 19(2) 2022, 37 – 43.

Science Letters

Impedance Data Interpretation for a Modified LSCF via Distribution of Relaxation Times Analyses

Suhaida Dila Safian[1*], Lidyayatty Malik[1] and Nafisah Osman[1,2]

[1]*Faculty of Applied Sciences, Universiti Teknologi MARA, 02600 Arau, Perlis, Malaysia*
[2] *Proton Conducting Fuel Cell Research Group, Faculty of Applied Sciences, Universiti Teknologi MARA, 40450 Shah Alam, Selangor, Malaysia*

ARTICLE INFO

Article history:
Received 9 October 2024
Revised 17 December 2024
Accepted 13 May 2025
Published 27 June 2025

Keywords:
Area Specific Resistance
Ba(Ce,Zr)O3, Distribution
LSCF
Relaxation Times

DOI:
10.24191/scl.v19i2.6868

ABSTRACT

Lanthanum Strontium Cobalt Ferrite Oxide (LSCF) is a cathode material for intermediate-temperature solid oxide fuel cells operating from 500 to 800 °C. To enhance the cathode's performance, it is essential to comprehend the electrochemical behavior, which is frequently analyzed using complex nonlinear least-squares (CNLS) analysis. Nevertheless, this analysis demonstrates certain constraints in the detailed interpretation of the electrochemical processes, particularly at the electrode-electrolyte interface. The distribution of relaxation times (DRT) is supportive when deconvoluting complex impedance spectra and has gained increased attention. Hence, this study is conducted to measure the electrochemical impedance data analyses by CNLS and the DRT of a fabricated modified 25 mm symmetrical cell, m-LSCF|BCZY|m-LSCF (m=modified, LSCF = $La_{0.6}Sr_{0.4}Co_{0.2}Fe_{0.8}O_3$ and BCZY = $BaCe_{0.54}Zr_{0.36}Y_{0.1}O_{2.95}$). In a Nyquist plot, the cell shows depressed semi-circles, representing a few interface processes occur. The DRT analysis reveals the semi-circles consisting of four different sub-processes (represented by four peaks) than CNLS (represented by four impedance arcs). The results show that the area-specific resistance (ASR) values for CNLS were 0.3 Ωcm^2 and 0.75 Ωcm^2, with 0.25 Ωcm^2 and 0.71 Ω cm^2 for DRT analysis.

INTRODUCTION

Proton ceramic fuel cells (PCFCs) are a subcategory of solid oxide fuel cells (SOFCs) that have seen increased attention in recent years [1]. These fuel cells can turn the hydrogen fuel into hydrogen ions with higher efficiency compared to engines and thermal power plants. The oxidation of hydrogen gas into hydrogen ions at the anode side and the reduction of oxygen ions at the cathode side, produces water as a byproduct. Compared to SOFCs with oxygen ion-conducting electrolytes, PCFCs have two key advantages:

[1*] Corresponding author. *E-mail address*: suhaidadila@uitm.edu.my
https://doi.org/10.24191/scl.v19i2.6868

first, protons are smaller than oxygen ions and can migrate through the electrolyte more easily at intermediate operating temperatures (500-800 °C); second, during operation, water vapors are formed at the cathode. This allows for better utilization of the fuel and removal of the product. The performance of PCFCs must be enhanced, and one way to do so is by investigating new or modified cathode materials, as the operating principles of PCFCs differ from those of oxygen ion SOFCs and the operating temperature is generally lower.

Lanthanum strontium cobalt ferrite (LSCF) is a widely used cathode in SOFC/PCFC technology [2]. This material is chosen for its elevated mixed ionic-electronic conductivity (MIEC), excellent ORR catalytic activity, compatibility with various electrolytes, and high ionic and electrical conductivity ($1x10^{-2}$ and 10^2 Scm^{-1} at 800 °C respectively). The comprehension of the reaction sites on the LSCF cathode has recently attracted substantial attention to improving the conductivity of the LSCF [3]. However, one of the most significant challenges in the development of LSCF is the lack of long-term durability, which is essential for commercialization, due to LSCF deterioration induced by strontium (Sr) surface segregation [4]. Surface strontium segregation of the A-site, which occurs frequently in Sr-containing perovskite-based electrodes such as LSCF and LSC, can reduce electrochemical activity for oxygen reduction reactions (ORR). This is due to elastic energy minimization and electrostatic or charge interactions from lattice mismatches between the dopant and the host, which causes Sr segregation [5]. As a result, many existing studies focus on reducing the negative effects of Sr segregation [6 - 9] by surface decoration using metal cations (Hf^{4+}, Ti^{4+}, Zr^{4+}) that may contribute to better surface stability against Sr segregation. This surface modification is important in increasing ORR activity and hence minimizing harmful cation segregation [10].

Electrochemical impedance spectroscopy (EIS) is a highly effective technique for analyzing intricate electrochemical systems in SOFC. This approach exploits the disparity in time constant and frequency response of the polarization loss mechanism occurring in an electrochemical system [11], [12]. The impedance spectra are evaluated by an equivalent circuit model (ECM) using complex non-linear least-squares (CNLS) fit model functions [13]. However, impedance data fitting using CNLS becomes challenging as some impedance patterns for actual electrochemical responses are almost or partially overlayed [14, 15].

Analyzing the electrode dispersions is not a simple task, in which the ECM must be seen as a global approximation of the electrochemical transport and transfer process. Therefore, to overcome these limitations, the deconvolution distribution of relaxation time (DRT) has attracted significant attention recently for interpreting EIS data or assisting the design of ECMs without a priori assumptions [16, 17]. DRT is a well-established method for deconvoluting EIS data from a fuel cell, in which it provides a deeper insight into electrode reactions and supports the identification of the most accurate ECM. The number of electrochemical processes and their characteristic relaxation times can be ascertained from the DRT spectrum. Moreover, DRT helps to identify an equivalent circuit that should be used to fit impedance data.

EXPERIMENTAL

Sample preparation

The respective $BaCe_{0.54}Zr_{0.36}Y_{0.1}O_{2.95}$ (BCZY) and $La_{0.6}Sr_{0.4}Co_{0.2}Fe_{0.8}O_3$ (LSCF) powders were prepared using a sol-gel method dissolving nitrate salts of barium, ($Ba(NO_3)_2$) (99% purity, ACROS); cerium (III) nitrate hexahydrate, $Ce(NO_3)_3.6H_2O$ (99.5% purity, ACROS); Zirconyl (IV) nitrate hydrate, $Zr(NO_3)_2O.xH_2O$ (99.5% purity, ACROS); Yttrium (III) nitrate hexahydrate, $Y(NO_3)_3.6H_2O$ (99.9% ACROS) and Lanthanum (III) nitrate hexahydrate, $La(NO_3)_3.6H_2O$ (99.95% purity, ACROS); Strontium nitrate, $Sr(NO_3)_2$, (99% purity, ACROS); Cobalt (II) nitrate hexahydrate, $Co(NO_3)_2.6H_2O$ (99% purity, ACROS) and Iron (III) nitrate nanohydrate $Fe(NO_3)_3.9H_2$) (99% purity, ACROS) in aqueous solution at

https://doi.org/10.24191/scl.v19i2.6868

room temperature with the addition of complexing agents like EDTA ($C_{10}H_{16}N_2O_8$: 99% purity, ACROS), citric acid ($C_6H_8O_7.H_2O$): 99.5% purity, MERCK), and ethylene glycol (ACROS). The mixture went through a few steps of different heat profiles in which a calcination temperature of 900 °C for LSCF and 1100 °C for BCZY was utilized to produce the single-phase cathode and electrolyte powders, as previously stated [18]. A 25-mm diameter and 1.3-mm thick BCZY pellet was produced using a dry pressing process with a pressure of 9 tons and a pressing period of 7 minutes. To densify the pellet, 4wt% of NiO was added to BCZY as a sintering aid [19]. The addition of the sintering aid was found to be very effective, yielding a relative density of 95% for the BCZY electrolyte.

The following describes the fabrication of a modified and unmodified 25 mm symmetrical cell with the configuration of m-LSCF/BCZY/m-LSCF (Cell A) and LSCF/BCZY/LSCF (Cell B) respectively. The cathode slurry was prepared by mixing the single-phase LSCF cathode powder with a binder solution at a ratio of 50:50. To remove organic binders and to generate close electrode-electrolyte attachment, the slurry was heated at 600 and 900 °C.

0.324 g of zirconium chloride ($ZrCl_4$) was dissolved in deionized water, stirred, and heated to 80 °C in order to modify the surface of Cell A. The LSCF thin film was submerged into the prepared solution and dried for 2 minutes. The Pt was manually pasted on both sides of the cells and utilized as a current collector.

The ZIVE SP2 Electrochemical Workstation (ZIVE LAB WonATech) was employed to investigate the electrochemical performance of the cell in stagnant air. The perturbation amplitude was set to 10 mV, and the frequency range was 10 mHz–1 MHz. Both cells were stabilized at 800 °C to preserve stability at the electrochemical impedance spectroscopy (EIS) setpoint before applying the sinusoidal signals. After 34 hours of stabilization period, the impedance data were further collected at 750 °C. The ZMANTM 2.2 f3 (ZIVE LAB) software was used to perform fitting and modeling of the impedance data. The distribution of relaxation times (DRT) functions was determined using self-software packages that were compiled in MATLAB code and based on the Tikhonov regulation [20]. This DRT is plotted against the time constant, with the peaks representing the major time constant of the electrochemical system and the area under each peak representing the polarization resistance (R_p) of a sub-process in the electrochemical response.

RESULTS AND DISCUSSION

The EIS spectra of Cell A and Cell B were acquired at 750 °C in the air with platinum (Pt) as a current collector and are presented in the form of a Nyquist plot as shown in Figure 1. The spectrum that consists of four depressed semicircles was then fitted with an equivalent circuit of L_s-R_s-$R_1|Q_1$-$R_2|Q_2$-$R_3|Q_3$-$R_4|Q_4$, in which L_s and R_s are the inductor and total ohmic resistance respectively, and R_1Q_1 (high frequency) – R_2Q_2 (medium frequency) – R_3Q_3 to R_4Q_4 (low frequency) correspond to electrolyte contribution (high frequency) and the cathode processes (medium to low frequency) as accordingly based on the Adler-Lane-Steele (ASL) [18]. The data indicate the equivalent circuit reflects four ORR contributions, which ultimately results in the overall cathodic resistance of the system. A cathode sample's performance is often assessed by measuring its polarization resistance, which is then reported in terms of area specific resistance (ASR). According to [20], the difference between the high-medium (1 MHz-1Hz) and low frequency (1 Hz-10 mHz) intercepts indicates polarization resistance, R_p, in which the Cell A spectrum is significantly smaller than Cell B, indicating a decrease in the R_p as the R_p represent the cathodic polarization resistance, calculated as the sum of R_1,R_2,R_3 and R_4 [21, 22].

The symmetrical cell of Cell A has an ASR of 0.3 Ωcm^2, which is significantly lower than Cell B's 0.75 Ωcm^2, as determined by the equivalent circuit and CNLS fitting. It can be noted that as a

https://doi.org/10.24191/scl.v19i2.6868

consequence of the surface decoration, the total cathode polarization is reduced by 60 %. The ASR obtained for Cell A is remarkably lower than pristine LSCF value of 0.61 Ωcm^2 as reported by Ismail et al. [23, 24]. The resistance of the cathode was significantly decreased by suppressing Sr segregation using the surface modification procedure. According to Tsvetkov et al. [25, 26] , surface modification by metal cations has decreased the negatively charged point defects of Sr that are caused by oxygen vacancies and a net positive charge at the perovskite surface. Details on the segregation and suppression of Sr segregation have been previously reported [27] .

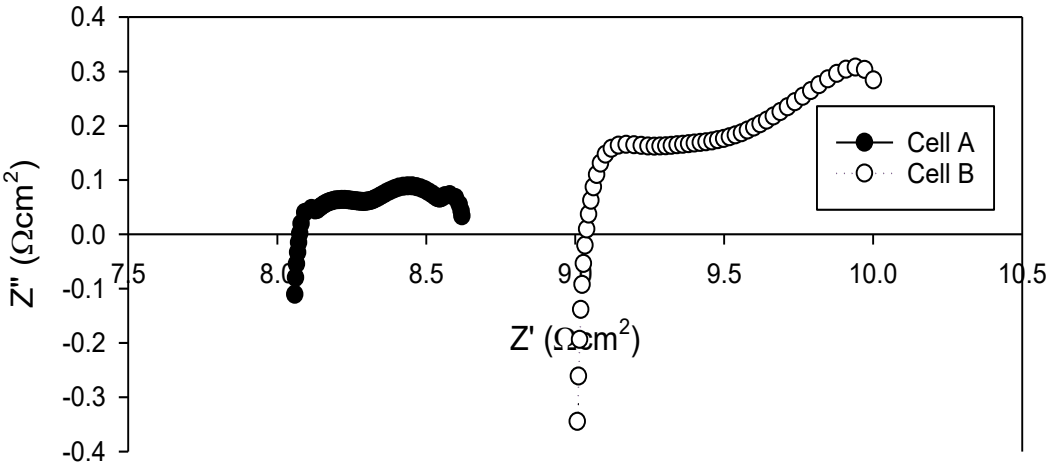

Figure 1. A Nyquist plot of Cell A and Cell B at 750 °C

Particularly, to understand the underlying reaction mechanism responses, the DRT functions are plotted as shown in Figure 2. The resultant DRT plots confirm that the cathodic process consists of four sub-processes (P_1, P_2, P_3, and P_4) ranging from high-medium to low frequency as reported previously [20]. Based on the high resolution of DRT curves, each deconvolution and the region under the peak represent the simulated resistance corresponding to the sub-process peak expressed in one certain reaction step for the cell's electrode reaction [17]. In other words, the smaller the peak area, the easier chemical processes will take place. The DRT analysis has confirmed the ASR of Cell A and B to be 0.25 and 0.71 Ωcm^2, respectively.

https://doi.org/10.24191/scl.v19i2.6868

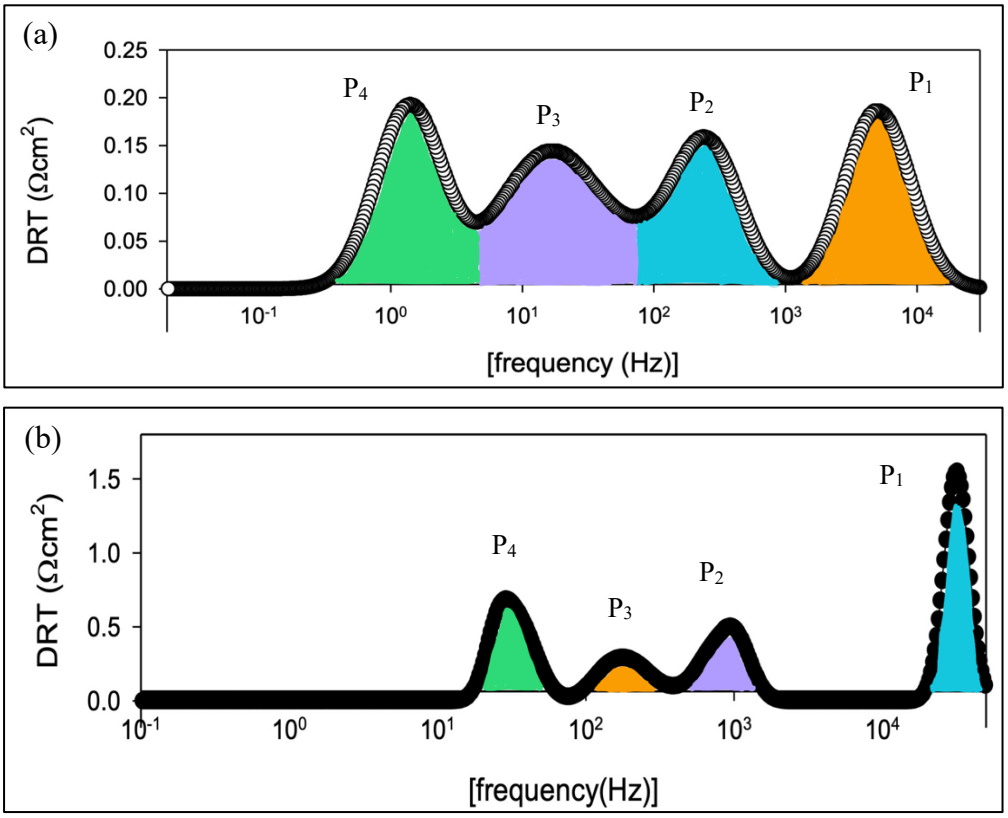

Figure 2. Corresponding DRT plots where four sub-processes (denoted as P_1, P_2, P_3 and P_4) for (a) Cell A and (b) Cell B

Additionally, the fundamental reaction mechanism and related responses are understood through the usage of the DRT functions [28]. As for LSCF cathode, P_1 sub-process is attributed to the electron transfer between the current collector and the cathode as mentioned previously by [29]. The P_2 and P_3 sub-process is reported associated with the oxygen ion transfer across the interface of cathode-electrolyte and the oxygen surface exchange process which comprises O_2 adsorption, dissociation an incorporation at cathode surface respectively. P_4, which can be observed at low frequencies, are indicative of the diffusion of oxygen gas throughout the whole cathode surface [30]. Therefore, the cathodic process in the respective frequencies can be identified through the use of DRT analyses, as the impedance arcs have been recognized for a long time as a result of a distribution of the time constant of electrical changes in the materials [31].

CONCLUSION

The electrochemical processes of LSCF|BCZY|LSCF symmetrical cells were investigated utilizing both CNLS and DRT analysis. The difficulty in distinguishing the processes through CNLS analysis is resolved using the DRT technique, in which the DRT analysis is more precise and easily reveals the semi-circles consisting of four different sub-processes that contribute to the cathode polarization resistance with cell A

https://doi.org/10.24191/scl.v19i2.6868

and cell B's ASR values from CNLS and DRT studies are nearly identical. Thus, the corroborated DRT with CNLS analysis properly defines PCFC-relevant EIS data.

ACKNOWLEDGMENTS

This work was supported by The Universiti Teknologi MARA (UiTM) via fundamental research grant scheme (FRGS) with reference no. 600-RMC/FRGS 5/3 (051/2024) and Dana Dalaman Grant UiTM with reference no. 600-UiTMPs (PJIM&A/UPP.5/2).

CONFLICT OF INTEREST STATEMENT

The authors agree that this research was conducted in the absence of any self-benefits, commercial or financial conflicts and declare the absence of conflicting interests with the funders.

REFERENCES

[1] C. Duan, J. Huang, N. Sullivan, and R. O'Hayre, "Proton-conducting oxides for energy conversion and storage," *Appl. Phys. Rev.*, vol. 7, no. 1, 2020, doi: 10.1063/1.5135319.

[2] S. P. Jiang, "Development of lanthanum strontium cobalt ferrite perovskite electrodes of solid oxide fuel cells – A review," Mar. 15, 2019, *Elsevier Ltd*. doi: 10.1016/j.ijhydene.2019.01.212.

[3] N. A. Baharuddin, H. A. Rahman, A. Muchtar, A. B. Sulong, and H. Abdullah, "Development of lanthanum strontium cobalt ferrite composite cathodes for intermediate- to low-temperature solid oxide fuel cells," *J. Zhejiang Univ. Sci. A*, vol. 14, no. 1, pp. 11–24, Jan. 2013, doi: 10.1631/jzus.a1200134.

[4] W. Araki, T. Yamaguchi, Y. Arai, and J. Malzbender, "Strontium surface segregation in La<inf>0.58</inf>Sr<inf>0.4</inf>Co<inf>0.2</inf>Fe<inf>0.8</inf>O<inf>3 -δ</inf> Annealed under compression," *Solid State Ionics*, vol. 268, no. Part A, pp. 1–6, Dec. 2014, doi: 10.1016/j.ssi.2014.09.019.

[5] Y. Yu, "Surface Segregation in Strontium Doped Lanthanum Cobalt Ferrite: Effect of Composition, Strain and Atmospheric Carbon Dioxide," *Ph.D. Thesis, Bost. Univ.*, 2016.

[6] T. S. Bjørheim, M. Arrigoni, S. W. Saeed, E. Kotomin, and J. Maier, "Surface Segregation Entropy of Protons and Oxygen Vacancies in BaZrO3," *Chem. Mater.*, vol. 28, no. 5, pp. 1363–1368, Mar. 2016, doi: 10.1021/acs.chemmater.5b04327.

[7] W. L. and B. Yildiz, "Factors that Influence Cation Segregation at the Surface of Perovskite Oxides," *J. Chem. Inf. Model.*, vol. 53, no. 9, pp. 1689–1699, 2018, doi: 10.1017/CBO9781107415324.004.

[8] J. Yang, L. Chen, D. Cai, H. Zhang, J. Wang, and W. Guan, "Study on the strontium segregation behavior of lanthanum strontium cobalt ferrite electrode under compression," *Int. J. Hydrogen Energy*, vol. 46, no. 15, pp. 9730–9740, 2021, doi: 10.1016/j.ijhydene.2020.12.228.

[9] K. Chen and S. P. Jiang, *Surface Segregation in Solid Oxide Cell Oxygen Electrodes: Phenomena, Mitigation Strategies and Electrochemical Properties*, no. August. Springer Singapore, 2020. doi: 10.1007/s41918-020-00078-z.

[10] H. Chen *et al.*, "Improving the Electrocatalytic Activity and Durability of the La0.6Sr0.4Co0.2Fe0.8O3-δ Cathode by Surface Modification," *ACS Appl. Mater. Interfaces*, vol. 10, no. 46, pp. 39785–39793, 2018, doi: 10.1021/acsami.8b14693.

[11] J. Xia, C. Wang, X. Wang, L. Bi, and Y. Zhang, "A perspective on DRT applications for the analysis

of solid oxide cell electrodes," *Electrochim. Acta*, vol. 349, p. 136328, 2020, doi: 10.1016/j.electacta.2020.136328.

[12] J. J. Giner-Sanz, E. M. Ortega, M. García-Gabaldón, and V. Pérez-Herranz, "Theoretical Determination of the Stabilization Time in Galvanostatic EIS Measurements: The Simplified Randles Cell," *J. Electrochem. Soc.*, vol. 165, no. 13, pp. E628–E636, 2018, doi: 10.1149/2.0271813jes.

[13] B. A. Boukamp, "Distribution (function) of relaxation times, successor to complex nonlinear least squares analysis of electrochemical impedance spectroscopy?," *JPhys Energy*, vol. 2, no. 4, 2020, doi: 10.1088/2515-7655/aba9e0.

[14] D. A. Osinkin, "An approach to the analysis of the impedance spectra of solid oxide fuel cell using the DRT technique," *Electrochim. Acta*, vol. 372, p. 137858, 2021, doi: 10.1016/j.electacta.2021.137858.

[15] A. L. Gavrilyuk, D. A. Osinkin, and D. I. Bronin, "On a variation of the Tikhonov regularization method for calculating the distribution function of relaxation times in impedance spectroscopy," *Electrochim. Acta*, vol. 354, p. 136683, 2020, doi: 10.1016/j.electacta.2020.136683.

[16] D. A. Osinkin, "Detailed analysis of electrochemical behavior of high–performance solid oxide fuel cell using DRT technique," *J. Power Sources*, vol. 527, no. February, p. 231120, 2022, doi: 10.1016/j.jpowsour.2022.231120.

[17] Y. Wang, B. Marchetti, and X. D. Zhou, "Call attention to using DRT and EIS to quantify the contributions of solid oxide cell components to the total impedance," *Int. J. Hydrogen Energy*, vol. 47, no. 83, pp. 35437–35448, Oct. 2022, doi: 10.1016/j.ijhydene.2022.08.093.

[18] N. I. A. Malek, I. Ismail, A. M. M. Jani, and N. Osman, "Characterization of LaSrCoFeO3 cathode material prepared with the aid of functionalized carbon nanotubes for proton conducting fuel cell," in *AIP Conference Proceedings*, 2020. doi: 10.1063/5.0003788.

[19] L. Bi, S. P. Shafi, E. H. Da'as, and E. Traversa, "Tailoring the Cathode–Electrolyte Interface with Nanoparticles for Boosting the Solid Oxide Fuel Cell Performance of Chemically Stable Proton-Conducting Electrolytes," *Small*, vol. 14, no. 32, pp. 1–9, 2018, doi: 10.1002/smll.201801231.

[20] S. D. Safian *et al.*, "Lanthanum-Ferrite based cathode: Impedance data interpretation via complex nonlinear least-squares and distribution of relaxation times analyses," *Ceram. Int.*, vol. 50, no. 20PC, pp. 40518–40525, 2024, doi: 10.1016/j.ceramint.2024.05.446.

[21] C. Lei, M. Simpson, and A. Virkar, "Measurement of Polarization Resistances of LSCF/YSZ/LSCF Symmetrical Cell Using Alternating Current (AC) and Direct Current (DC) Techniques," *ECS Meet. Abstr.*, vol. MA2021-02, no. 42, pp. 1294–1294, Oct. 2021, doi: 10.1149/MA2021-02421294mtgabs.

[22] H. Sumi *et al.*, "External Current Dependence of Polarization Resistances for Reversible Solid Oxide and Protonic Ceramic Cells with Current Leakage," 2023, doi: 10.1021/acsaem.2c03733.

[23] I. Ismail, N. Osman, and A. M. M. Jani, "Evaluation of La0.6Sr0.4Co0.2Fe0.8O3-δ as a potential cathode for proton-conducting solid oxide fuel cell," *Sains Malaysiana*, vol. 47, no. 2, pp. 387–391, Feb. 2018, doi: 10.17576/jsm-2018-4702-21.

[24] I. Ismail, A. M. M. Jani, and N. Osman, "Microstructure control of SOFC cathode material: The role of dispersing agent," in *AIP Conference Proceedings*, American Institute of Physics Inc., Sep. 2017. doi: 10.1063/1.4999860.

[25] N. Tsvetkov, Q. Lu, L. Sun, E. J. Crumlin, and B. Yildiz, "Improved chemical and electrochemical stability of perovskite oxides with less reducible cations at the surface," *Nat. Mater.*, vol. 15, no. 9,

https://doi.org/10.24191/scl.v19i2.6868

pp. 1010–1016, Sep. 2016, doi: 10.1038/nmat4659.

[26] N. Tsvetkov, Q. Lu, and B. Yildiz, “Improved electrochemical stability at the surface of La $_{0.8}$ Sr $_{0.2}$ CoO $_{3}$ achieved by surface chemical modification,” *Faraday Discuss.*, vol. 182, pp. 257–269, 2015, doi: 10.1039/C5FD00023H.

[27] S. D. Safian, N. I. Abd Malek, Z. Jamil, S. W. Lee, C. J. Tseng, and N. Osman, “Study on the surface segregation of mixed ionic-electronic conductor lanthanum-based perovskite oxide La1−xSrxCo1−yFeyO3−δ materials,” *Int. J. Energy Res.*, no. January, pp. 1–17, 2022, doi: 10.1002/er.7733.

[28] C. Plank *et al.*, “A review on the distribution of relaxation times analysis: A powerful tool for process identification of electrochemical systems,” *J. Power Sources*, vol. 594, no. November 2023, p. 233845, 2024, doi: 10.1016/j.jpowsour.2023.233845.

[29] C. Y. Yoo *et al.*, “Investigation of Electrochemical Properties of Model Lanthanum Strontium Cobalt Ferrite-Based Cathodes for Proton Ceramic Fuel Cells,” *Electrocatalysis*, vol. 7, no. 4, pp. 280–286, 2016, doi: 10.1007/s12678-016-0306-1.

[30] J. Li *et al.*, “Suppressing surface segregation by introducing lanthanides to enhance high-temperature oxygen evolution reaction activity and durability,” *JPhys Energy*, vol. 7, no. 2, 2025, doi: 10.1088/2515-7655/ada4dc.

[31] K. Dumaisnil, J. C. Carru, D. Fasquelle, M. Mascot, A. Rolle, and R. N. Vannier, “Promising performances for a La0.6Sr0.4Co0.8Fe0.2O3-δ cathode with a dense interfacial layer at the electrode-electrolyte interface,” *Ionics (Kiel).*, vol. 23, no. 8, pp. 2125–2132, 2017, doi: 10.1007/s11581-017-2061-6.

https://doi.org/10.24191/scl.v19i2.6868